

Wide Bandwidth Fixture De-Embedding Achievable Through Use of a Single Calibration Structure

Brandon W. Ardisson, School of Electrical, Computer and Energy Engineering, Arizona State University, Tempe, AZ USA

Abstract—This work will introduce the IEEE P370 standard and examine one of the PCB fixture de-embedding techniques detailed in this specification, the 2x Thru calibration. The Qorvo TQP3M9035 LNA and its accompanying characterization board will serve as the device under test (DUT). This device’s S parameters will be measured and subsequently de-embedded. 2x Thru de-embedding will be performed using the standard’s prescribed algorithm and also using Keysight’s proprietary 2x Thru AFR algorithm. The effectivity and accuracy of these de-embedding techniques will be summarized through analysis and comparison of the measured, 2x Thru de-embedded, and manufacturer provided S parameter datasets.

Index Terms—Calibration, fixtures, integrated circuit measurements, measurement techniques, microwave measurement, millimeter wave measurements, parameter extraction, radiofrequency integrated circuits, scattering parameters, verification.

I. INTRODUCTION

When performing MMIC device characterization, PCB test fixtures are something that every engineer needs, but does not want. These test fixtures are necessary, as they provide the physical structure for the transmission line, routing signals out from the MMIC package to the coaxial connector, a common point of connection for high frequency test and measurement equipment.

These PCB test fixtures cloud the performance of the DUT by introducing error terms that accompany the additional transmission line and interconnect structures. The error terms introduced stem from parasitic capacitances and inductances that result in impedance variations along the signal path. These errors need to be removed from the measurement either in real time or through post-processing. The removal of these error terms is performed in a process called de-embedding. This process is necessary to ensure that the measured performance correctly represents the performance of the DUT. Just as VNA calibration moves the measurement reference plane to the end of the coaxial connector, de-embedding moves the reference plane from the coaxial interconnect right up to the DUT package. As seen in Figure 1, the fixture to be de-embedded is found between each set of dashed lines.

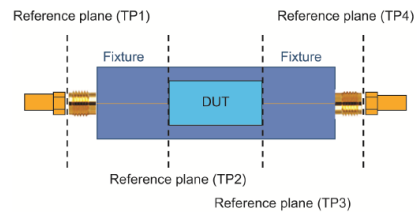


Figure E.1—Coaxial connectors on a printed circuit board (PCB) with microstrip traces connected to a DUT

Figure 1: Identifying fixture bounds for second tier calibration
Source: Adapted from [1].

Test fixture transmission lines and interconnects can be modeled using a 3D field simulator such as HFSS or CST, but these models do not account for the non-idealities that result from manufacturing or assembly variance. When high accuracy is needed, it is common to utilize the SOL or TRL de-embedding techniques by building the required calibration structures on the test fixture PCB, or fabricating a dedicated PCB for this purpose. This ensures that the calibration structures “see” the same non-idealities as the DUT signal paths and can compensate for them during the de-embedding procedure.

De-embedding algorithms such as SOL and TRL are mathematically perfect. Simulation shows how de-embedding can remove complex test fixtures without error. However, in a real test environment, error can result due to poor measurements and variations between the calibration standards and their theoretical ideals [2]. Other limitations to these de-embedding methods come from that practicality of implementation. For high pin count / multi-port devices it is cost and size prohibitive to implement multiple calibration structures for each DUT port that needs to be de-embedded. Increasing the calibration structure count also increases the likelihood of user error.

The IEEE 370 standard introduced in September 2020 addresses some of these concerns. The standard’s abstract states its primary goal, “This document provides standard practices for ensuring the quality of measured data for high-frequency electrical interconnects at frequencies up to 50 GHz.” [1:13]. In particular, recommended test fixture design, de-embedding techniques, and measurement procedures that ensure accuracy and consistency are detailed. Although the title of the standard states a frequency maximum of 50 GHz, the standard and general practice should also be applicable for frequencies higher than 50 GHz [1].

Of specific interest is the 2x Thru de-embedding method detailed in Annex D of the standard. For RFIC devices with multiple RF ports, full fixture de-embedding is necessary to correlate device performance with simulation. The 2x Thru method has been shown to produce results that are equivalent or better than those obtained using TRL calibration [1]. This is an attractive method because only a single calibration structure is required to de-embed a 2 port device.

Additionally, this single calibration structure does not rely on fabrication of an ideal standard such as an open, short, or load.

Understanding, implementing, and utilizing this de-embedding method has the potential to reduce test fixture cost, reduce likelihood of measurement error, and increase the accuracy of DUT characterization. Realizing these improvements can enable design teams to more closely correlate simulations and ultimately reduce the number of design cycles required to ascertain desired device performance.

II. MATERIALS AND METHODS

The recommended implementation of the 2x Thru de-embedding structure can be seen below in Figure 2. The name 2x Thru indicates that the de-embedding structure is formed by connecting both port 1 and port 2 transmission lines (of equal length) to form a single thru transmission line that is twice the length of the transmission line feeding either port.

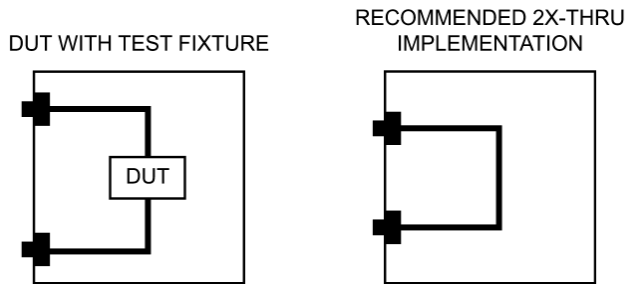


Figure 6—2X-Thru implementation

*Figure 2: IEEE P370 2x Thru Recommended Implementation
Source: Adapted from [1].*

When implementing the 2x Thru de-embedding structure onto PCB, it is important to use end launch coaxial connectors and transmission line geometries that are identical to those that connect to the DUT. Due to the small size and large bandwidth of this single de-embedding structure, it can easily be fabricated on the same PCB as the DUT. This ensures that PCB manufacturing and processing variations are the same amongst the actual transmission line and the de-embedding structures.

Regarding resolution and bandwidth of the 2x Thru, section 4.3.11 of [1] specifies a minimum length of the de-embedding structure. The 2x Thru de-embedding method uses FFT to convert frequency domain S-Parameters into a time-domain reflectometry/transmissometry (TDR/TDT) waveform. Per the standard, in order to have enough resolution, the length of the 2x Thru should be at least three wavelengths long at the highest frequency to be measured. For the same reason, Keysight's AFR standard will specify that the Thru be four times the signal

rise time [5].

The theory behind the 2x Thru (and AFR) technique, as alluded to, involves utilizing information about the S-Parameters in the time domain to provide information about the missing error term.

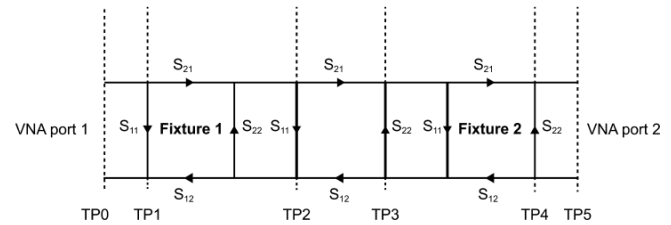
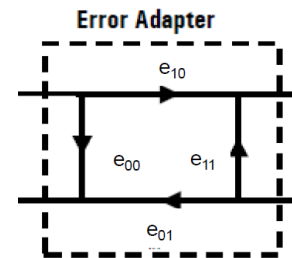


Figure E.3—Measurement diagram with test points

Figure 3: Signal flow graph equivalent of Figure 1

We begin the de-embedding by identifying that each fixture to be de-embedded is fully described by its own set of S-Parameters. To better align with the fact that each fixture's S-Parameters contribute to the error of the S-Parameters of the DUT, we classify each fixture (seen above in Figure 3) as an error adapter. The error terms of each adapter can be found by measuring the S-Parameter response and solving for each error term using the equations derived from the signal flow graph of the structure.



*Figure 4: Error adapter and associated terms e_{xx} .
Source: Adapted from [3].*

Following the signal flow graph analysis of the adapter in [4], we can derive two transmission equations by inspection. This is done with the assumption that the error box is reciprocal, that is $e_{01} = e_{10}$.

$$T_{11} = e_{00} + \frac{e_{11} \cdot e_{01}^2}{1 - e_{11}^2}$$

$$T_{12} = \frac{e_{01}^2}{1 - e_{11}^2}$$

Figure 5: Derived T_{11} and T_{12} equations for the error adapter.

An issue arises due to the fact that only a single thru de-embedding structure is analyzed. We have only two equations and need to solve for three unknown values. We are unable to solve this without more information to provide for e_{00} . To work around this problem, we use our knowledge of the de-embedding structure symmetries and delay information from the time domain response of the structure.

This information is found by bringing T_{12} into the time domain and calculating its step response. We can identify the

end of T_{12} in the time domain by finding the peak of its response [5]. Using the same method, we calculate or measure, the step response of T_{11} . Knowledge of a matched length thru structure, implies that the delay of the T_{11} is twice its length. Using this, we also now know the midpoint of the T_{12} response. With this information, zero padding is applied to all data points after T_{11} 's midpoint and the impulse response of this data is converted back to the frequency domain. This newly brought over information is in fact e_{00} , which was previously the missing error term [2].

This is the core working methodology which allows the IEEE 370 2x Thru de-embedding technique to achieve wide bandwidth performance with a single calibration structure. This is also the working technique behind Keysight's AFR (Automated Fixture Removal) technology, patented by Dunsmore in 2014 [5]. More information on this technique can be found in [5].

Once, the error adapter T-Parameters are found we can fully de-embed the DUT by measuring the Fixture-DUT-Fixture T-Parameters and then matrix multiply by the inverse T-Parameters of the error adapters, as shown in Figure 6.

$$T_D = T_F^{-1} T_{FDF} T_F^{-1}$$

where

T_D is the DUT T-parameters

T_F is the fixture model T-parameters

T_{FDF} is the Fixture-DUT-Fixture T-parameters

Figure 6: Application of matrix multiplication to de-embed the DUT.

To facilitate this experiment, I chose to utilize a readily available microwave low-noise amplifier evaluation board, the TQP3M9035-PCB. This component was chosen because the evaluation PCB already contained a dedicated calibration path that matched the implementation requirements for the 2x Thru de-embedding structure.

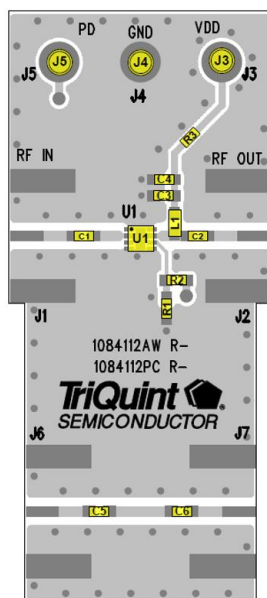


Figure 7: Capture of the layout for the TQP3M9035-PCB

To accommodate the short fixture length and the minimum length requirements of the de-embedding structure, characterization was performed from 10 MHz to 18.010 GHz. Using this high frequency span was necessary to perform accurate de-embedding. The high bandwidth allows for the use of a very fine pulse excitation in the time domain.

A Keysight PNA-X, 4 port vector network analyzer was utilized to perform the device characterization. Tier 1 calibration was performed using a properly calibrated E-Cal module, average power sensor, and torque wrench. Beyond the Tier 1 calibration point were 1.85mm to 2.92mm adapters which allowed for connection to the DUT fixture SMA coaxial connectors. These adapters were not included in the Tier 1 calibration and are considered to be included as part of the DUT fixture.

A small number of averaging iterations was applied, along with a reduced IFBW of 1 kHz. This provided for good dynamic range, a low noise floor, and smooth data acquisition. A capture of the complete test setup can be seen in Figure 8.



Figure 8: Photo of the test setup.

In order to perform the IEEE 370 standard 2x Thru de-embedding, post processing of measurement data was performed using MATLAB code that was provided as part of the standard [1]. The MATLAB post-processing created S-parameters for each fixture error box by using the 2x Thru S-Parameter measurements captured in the test data. Then these error box S-Parameters, along with the measured Fixture-DUT-Fixture parameters, were fed into another function that performed the de-embedding.

The Keysight AFR de-embedding was performed in situ by using the AFR application embedded within the PNA-X measurement equipment. In this case, the 2x Thru standard was measured and then the AFR algorithm was applied. Then the Fixture-DUT-Fixture measurements were made (keeping the AFR correction active). Both of the de-embedding methods directly provided S2P files at the outset, that could be readily viewed and analyzed.

To be clear, the IEEE 370 standard de-embedding method calculates the step response and performs time domain calculations during the post-processing step. Keysight’s AFR method actually performs the TDR excitation and time domain calculations during device measurement.

To indicate the performance of the de-embedding techniques, I requested fully de-embedded device parameter files from the device manufacturer, Qorvo. This data provided was performed by Qorvo on a different PCB test structure and utilized TRL to de-embed the intrinsic device characteristics. This data, along with my measured, and both sets of de-embedded data was overlaid onto a S-Parameter plot for visual analysis.

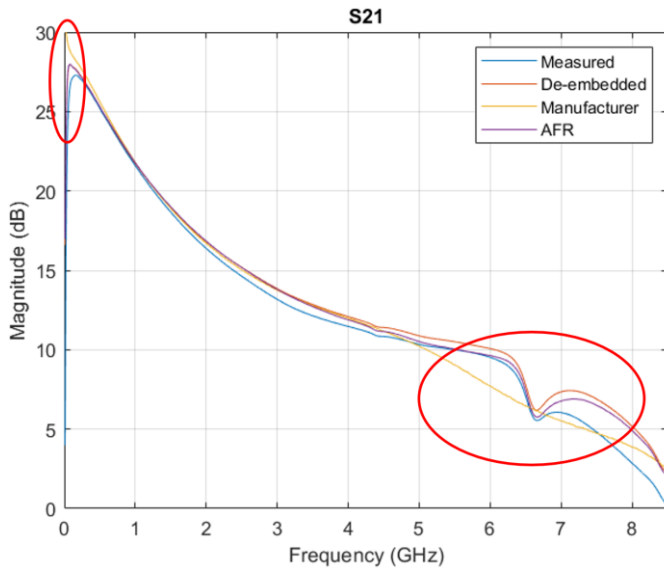


Figure 9: S21 of the measured and de-embedded datasets.

In Figure 9 we can see that, for the most part, both the IEEE 370 (titled “De-embedded”) and Keysight’s AFR de-embedding techniques match the manufacturer provided device parameters from about 500 MHz to 4 GHz. There are some obvious discrepancies at the upper and lower extremes of the measured frequency range. This can be attributed to differences between my test setup and the test setup used by the device manufacturer for their TRL calibration routine.

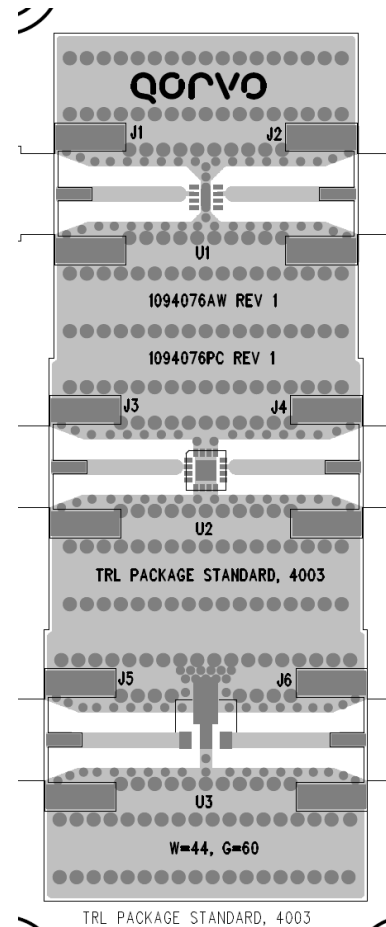


Figure 10: TRL Calibration PCB for the DUT. Source: Qorvo

For the most part, it is encouraging to see the close agreement between both the IEEE 370 2x Thru and Keysight’s AFR de-embedding tool.

The TRL calibration board used by the device manufacturer is shown in Figure 10. Noticeably absent are the series AC coupling capacitors and the biasing network on the device output. The series AC coupling capacitors will have a high impedance at low frequencies, this explains why my dataset sees a monotonic increase in gain until it reaches a maximum near 100 MHz. Since these capacitors were not present in the TRL calibration board, we see the manufacturer provided data peak near DC and monotonically decrease as frequency increases.

The deviation above 5 GHz can likely be attributed to resonant effects present at both the input and output of the DUT. The series AC coupling capacitors used in the TQP3M9035-PCB have a SRF between 500 MHz and 1 GHz. This implies that the capacitor will actually appear inductive beyond the SRF frequency. For the first few GHz the capacitors will be adding series resistance. Beyond this, their impedance grows in magnitude and could more easily interact with parasitic capacitances or the output biasing network of the DUT.

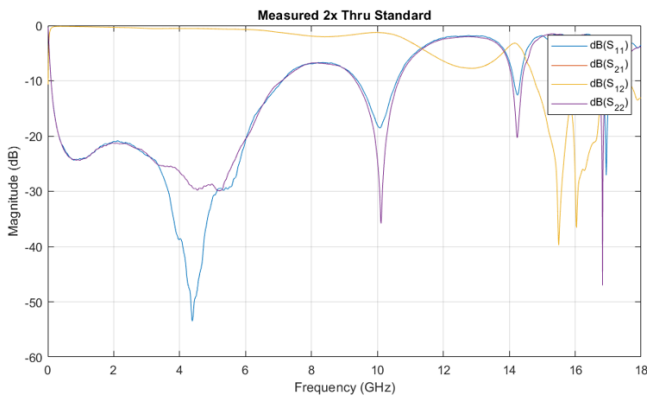


Figure 11: Measured 2x Thru Standard S-Parameters (not de-embedded).

This phenomenon is more plausible when we look at the asymmetries present between the S11 and S22 measurement data shown in Figure 11, specifically near 4.4 GHz. This indicates that the source impedance of the amplifier’s output, the output biasing network, and the series capacitor are indeed interacting with each other in a way that would not be realized on the manufacturer’s calibration board.

Figure 12 also reinforces this point by correlating the S21 and S22 datasets. We see that the S22 plot has a specific resonance at approximately 6.5 GHz. This frequency location is also where we see the step drop off in gain in Figure 9, suggesting that these two events are not independent. We can also see in Figure 12, that the IEEE 370 de-embedding method most closely tracked the actual S22 curve (titled “Manufacturer”) from near DC to about 4 GHz.

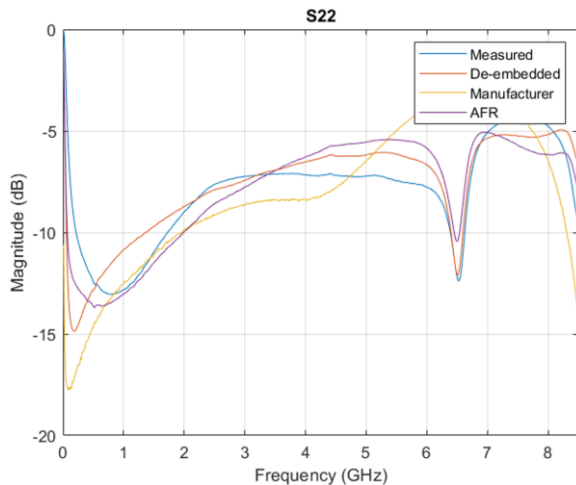


Figure 12: S22 of the measured and de-embedded datasets.

III. CONCLUSION

In conclusion, this work did show the correlation and agreement between the open source 2x Thru de-embedding technique described in IEEE 370, and the proprietary Keysight Automated Fixture Removal application; both methods tracked closely with each other. This gives more confidence to the user in the IEEE 370 method. The IEEE method being open source, is also more accessible since it does not require time domain reflectometry capabilities or additional software be added to existing VNA equipment.

While the IEEE 370 standard has been able to show that the 2x Thru de-embedding technique can achieve better than -20 dB absolute error, I was unfortunately unable to confirm that using this experiment. While I believe the de-embedded data that I have is accurate, I am unable to confirm since the manufacturer data used a different DUT configuration.

The TQP3M9035-PCB was a readily available and cost effective DUT that I believed would work to help me better characterize the discussed de-embedding techniques. Future work would involve modifying the DUT PCB to better match the manufacturer’s test setup. This would allow for the determination of the absolute error achievable with the 2x Thru method.

Now that I am more familiar with this style of de-embedding, I will likely continue further by focusing on the 1x Reflect de-embedding technique, which is also described in IEEE 370. This technique could be implemented without the need for any de-embedding structure, as it would use an open DUT transmission line as the calibration structure. This approach seems quite appealing for product development purposes.

Working through this project has increased my knowledge of current methods and practices. I have also learned to identify pitfalls and limitations that accompany this method in practical implementations.

REFERENCES

- [1] *IEEE Standard for Electrical Characterization of Printed Circuit Board and Related Interconnects at Frequencies up to 50 GHz*, IEEE 370, 2020.
- [2] J. Ellison, *Test-Fixture De-Embedding 101*, Signal Integrity Journal, June 28, 2017. Accessed on: March 7, 2021. [Online]. Available: <https://www.signalintegrityjournal.com/articles/463-test-fixture-de-embedding-101>
- [3] *Network Analyzer Basics*, 1st ed., Agilent Technologies, Santa Rosa, CA, USA, 2004, pp. 51-52.
- [4] D. M. Pozar, “Microwave Engineering”, 4th ed. Hoboken, NJ, USA: John Wiley & Sons, 2012, pp. 197-198.
- [5] J. P. Dunsmore, “Handbook of Microwave Component Measurements with Advanced VNA Techniques”, 2nd ed. Hoboken, NJ, USA, 2020, pp. 764-767.